POLISH MARITIME RESEARCH 1(64) 2010 Vol 17; pp. 51-56
10.2478/v10012-010-0005-4

Comparing N3-60 cascade exit angles obtained from tunnel measurements and numerical simulations

Biernacki Rafał, Ph. D.
Gdansk University of Technology
Piotr Krzyślak, Assoc. Prof.
Poznan University of Technology

ABSTRACT

The article compares the results of the measurements performed in the aerodynamic tunnel owned by the Czestochowa University of Technology and the numerical simulation done using the code FLUENT for a plane cascade of N3-60 profiles. The comparison study aims at assessing differences between the exit angles measured experimentally and those obtained from numerical calculations. Variable parameters in the measurements and the calculations were the relative pitch and the profile stagger angle. The measurements were performed in the flow of air. The same medium and having the same inlet parameters was assumed in the calculations. The calculations were performed in two dimensions for the compressible flow. The k-ε RNG turbulence model was used to complete the equation system. Comparing the measured and calculated results provides opportunities for assessing the range of differences between the experiment and the simulation. The obtained results and formulated conclusions will find the application not only in the power industry, but also in the shipbuilding industry for analysing the operation of steam and gas turbines used as main and auxiliary propulsion systems on both merchant vessels and battle ships.

Keywords: numerical calculations, profile characteristics, gas turbines, steam turbines

GEOMETRY OF N3 PROFILE

The N3-60 profile is a basic profile used in impulse turbines produced in Poland. In the eighties, a series of tests of those profiles were performed in the aerodynamic tunnel owned by the Czestochowa University of Technology. Variable parameters in these tests were the profile stagger angle α_u and the relative pitch t/b. The tests aimed at preparing basic flow characteristics of the profiles and cascades to use them in the turbine design process. An isolated profile N3 is shown in Fig. 1.

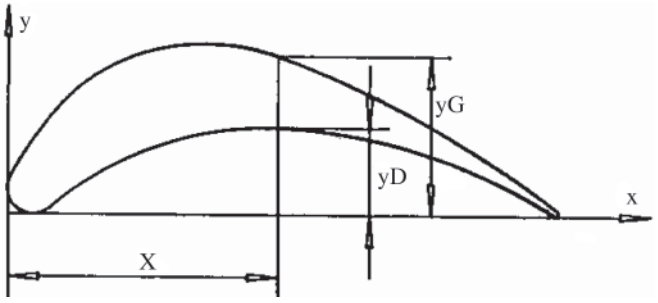

Fig. 1. *N3 profile contour lines [1]*

Basic geometrical parameters which define the N3-60 profile are given in Fig. 2. For the changing stagger angle α_u and the relative pitch t/b we can calculate the effective cascade exit angle, see the diagram in Fig. 3.

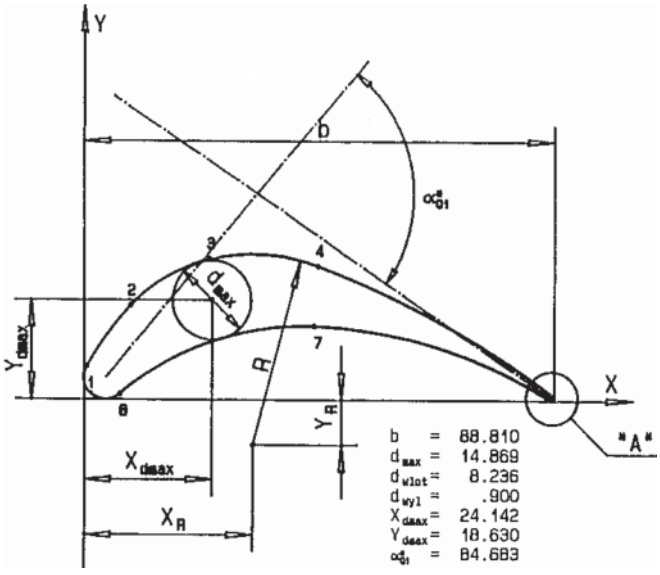

Fig. 2. *Geometrical parameters of N3-60 profile. [1]*

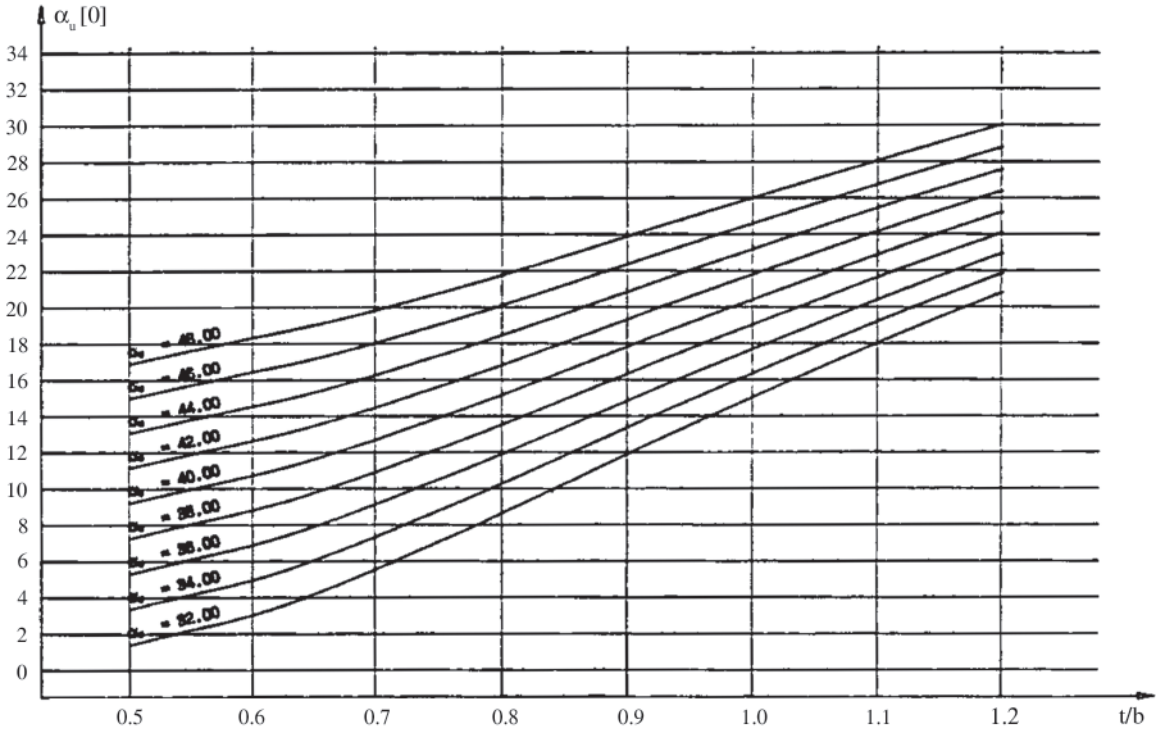

Fig. 3. *Effective N3-60 cascade exit angle [1]*

DISCUSSION OF THE EXISTING RESULTS OF N3 PROFILE MEASUREMENTS

The existing results of N3 profile measurements are published in [1]. The ranges of parameters changing in the profile tests were the following:

- relative pitch t/b - 0.5 to 1.2
- inlet flow angle - 45°, 75°, 90°, 120°
- cascade stagger angle - 34.6° to 48.6°
- inlet flow velocity - Ma = 0.2
- resultant Reynolds number - 0.38×10^6

The measured results, having the form of velocity distributions, were integrated and averaged to obtain one-dimensional characteristics of the cascade for the assumed profile stagger angle and pitch. The quantities determined in those measurements included the profile loss, the trailing edge loss, and the exit flow angle α_1. Fig. 3 shows the flow exit angle as a function of the relative pitch for the inlet flow angle α_0 equal to 90°. The basic goal of this study was to verify the differences between the real results obtained from the measurements and those calculated using the numerical model of the cascade.

AUTOMATION OF THE GEOMETRY GENERATION PROCESS

The profile co-ordinates were entered to the Excel calculation sheet. The entered data included fifty pairs of points in the Cartesian coordinate system which defined the upper and lower profile curve. The next step was to calculate the camber line, defined as:

$$x_s = x_g = x_d$$

$$y_s = 1/2(y_g + y_d)$$

For an arbitrary N3 profile stagger angle, the algorithm rotated the profile and its camber line using the following scheme:

$$x' = x\cos(\alpha) - y\sin(\alpha)$$

$$y' = x\sin(\alpha) + y\cos(\alpha)$$

After the rotation $x_g \neq x_d \neq x_s$. The passage axis was generated by shifting parallelly the camber line up and down by half of the assumed cascade pitch, and then extrapolated beyond the profile as the straight lines extending from x = -25 to x = 100. The input data for the geometry generation algorithm comprised a list of points which defined the profile in standard position, complemented by the rotation angle and the cascade pitch. Based on these data, the algorithm generated a script which introduced to the code Rhino a sequence of points describing the passage geometry after rotation and transformation. This method was used for creating a series of passage geometries taking into account diferent profile stagger angles and cascade pitches. Fig. 4 shows a sample geometry before and after the transformation for the stagger angle $\alpha = 44.58°$ and the relative pitch t/b = 0.6.

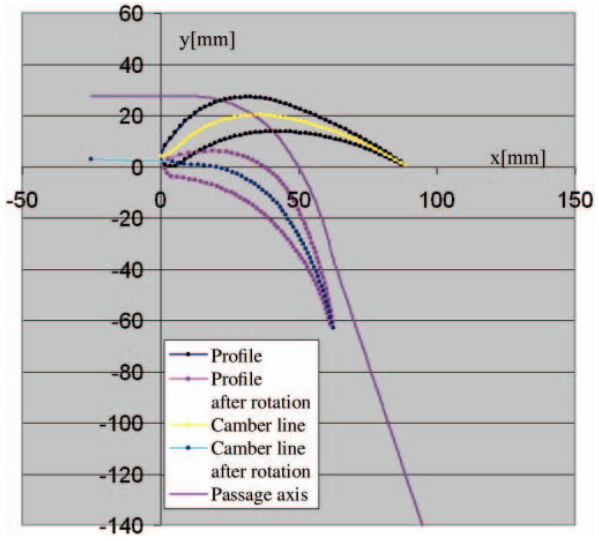

Fig. 4. *Profile transformation and creation of the passage axis*

The oriented N3 profile, mapped using the code Rhinoceros, was used as a basis for generating the calculation grid. The 2D calculation domain was bordered in front by a vertical inlet section, and at rear by a vertical exit section. From the top and the bottom the calculation domain was bordered by the axis of the blade-to-blade passage, treated as the border of periodical type.

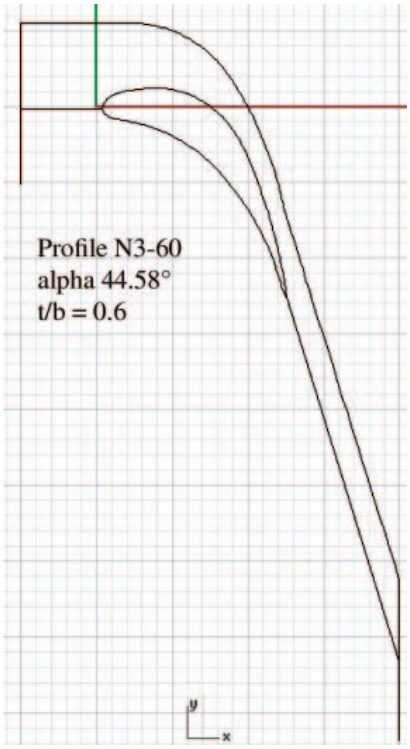

Fig. 5. *Geometry prepared for grid generation*

ASSUMPTIONS ADOPTED WHEN GENERATING THE CALCULATION GRID

In all cases, the geometry presented in the previous Section has made the basis for generating the calculation grid. The upper and lower boundaries of the calculation domain (see Fig. 5), which define the flow passage axis, were considered the periodic boundaries. The calculation domain was divided into two subdomains – over and below the plate, which made it possible to generate the boundary layer on the surface of the profile washed round by the flow . The calculation grids of structural type and dimensions 160 × 450 elements were generated automatically by the code, which made it possible to generate an optimised structure for each examined geometry variant. The generated grid was optimised with respect to the orthogonality of the gridlines. One of basic criteria for assessing the quality of the created grid was the minimum angle between the lines which limit the grid element.Tab.1 collects the values of the minimal angles for dif ferent calculation variants.

Tab. 1. *Minimal calculation grid angles*

		Profile stagger angle α_u			
		36.58	**40.58**	**44.58**	**48.58**
Cascade pitch t/b	**0.6**	3.06°	2.70°	3.55°	4.47°
	0.8	3.64°	3.44°	5.49°	6.44°
	1.0	3.91°	5.15°	6.89°	7.78°

Fig. 6 presents a sample calculation grid generated for the variant characterised by parameters: α_u = 44.58°, t/b = 0.6.

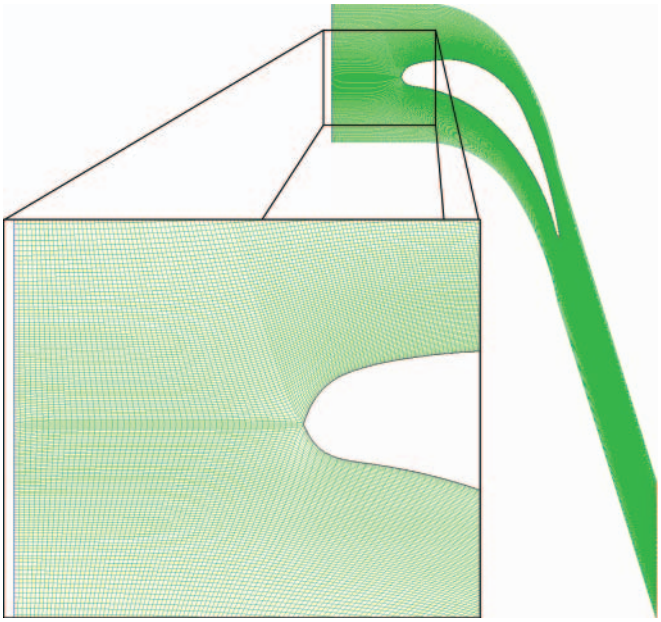

Fig. 6. *Sample calculation grid for N3-60 profile*

RANGE OF CALCULATIONS

The calculation grid similar to that shown in the precious Section was generated for each individual pair of profile stagger angle α_u and pitch t/b. The calculations done using these grids made use of parameters, the range of which is given in Tab. 2:

Tab. 2. *Range of parameters used in calculations*

		Profile stagger angle α_u			
		36.58	**40.58**	**44.58**	**48.58**
Cascade pitch t/b	**0.6**	☑	☑	☑	☑
	0.8	☑	☑	☑	☑
	1.0	☑	☑	☑	☑

The calculations were performed using the code Fluent [2]. The boundary conditions for all variants were taken from the experimental data. The assumed quantities included:

- mass flow rate through a single passage
- pressure at flow area exit
- type of working medium (the experiment was carried out for air)
- inlet temperature of the working medium
- model of fluid (viscous, compressible)
- turbulence model (k-ε RNG)
- values of turbulence parameters k and ε at passage inlet.

Part of the above parameters was constant for all calculated variants. This list includes: total inlet pressure assumed as equal to 100 kPa, inlet temperature of the working medium -300 K, and the model and parameters of the working medium. Boundary conditions which changed from variant to variant are given in Tab. 3.

Tab. 3. *Variable boundary conditions*

		$\dot{m}$ [kg/s]	**k** [m²/s²]	**ε** [m²/s³]
Cascade pitch t/b	**0.6**	2.480	21.627	2112.7
	0.8	3.307	21.627	1584.5
	1.0	4.133	21.627	1267.6

The values assumed in the calculations imitated the flow conditions recorded in the experiment.

SAMPLE RESULTS OF NUMERICAL CALCULATIONS

The obtained results of the calculations have made it possible to assess the effect of the distance of the test section from the trailing edge on the values of the exit angle $_1\alpha$. As could be expected, the calculated angle did not change much after leaving the profile cascade. Changes of this angle as a function of the distance from the blade trailing edge are shown in Fig. 7, for the selected sample pitch t/b = 0.6. When comparing with the results of the measurements, it was assumed that the distance from the trailing edge was equal to 5 mm.

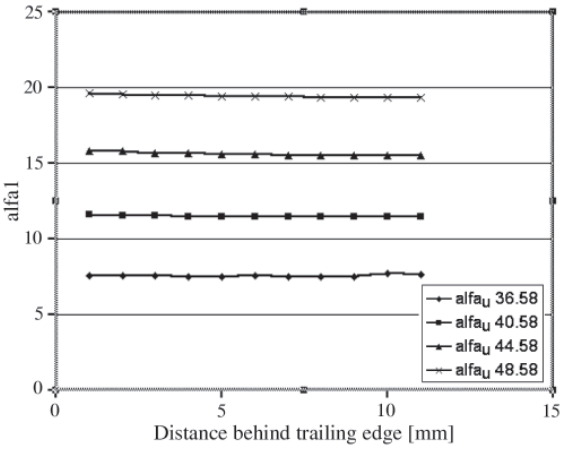

Fig. 7. The angle α_1 vs. the distance from the trailing edge

The next figures show the streamline and exit angle distributions in the calculation domain, as well as the exit angle distributions along the traverse line x = +5 mm downstream of the trailing edge.

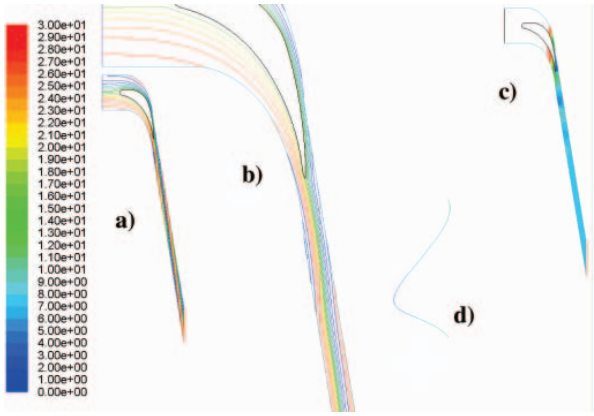

***Fig. 8.** Results of calculations for profile N3-60, α_u = 36.58°, t/b = 0.6; **a)** streamlines; **b)** streamlines – enlarged; **c)** exit angles (scale on the left); **d)** changes of exit angle α_1 along datum +5 mm*

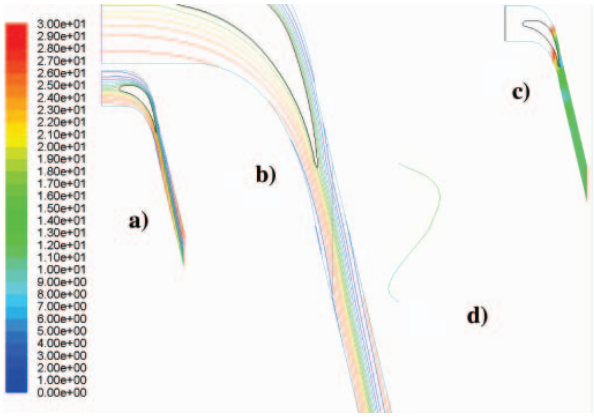

***Fig. 9.** Results of calculations for profile N3-60, α_u = 40.58°, t/b = 0.6; **a)** streamlines; **b)** streamlines – enlarged; **c)** exit angles (scale on the left); **d)** changes of exit angle α_1 along datum +5 mm*

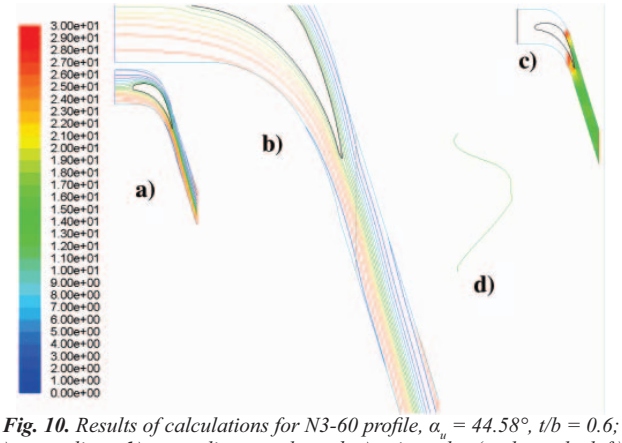

***Fig. 10.** Results of calculations for N3-60 profile, α_u = 44.58°, t/b = 0.6; **a)** streamlines; **b)** streamlines – enlarged; **c)** exit angles (scale on the left); **d)** changes of exit angle α_1 along datum +5 mm*

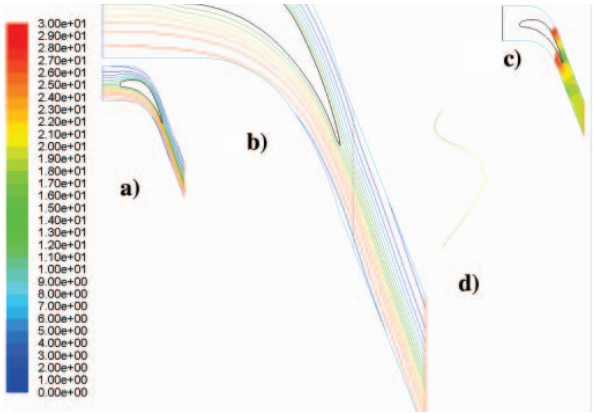

***Fig. 11.** Results of calculations for profile N3-60, α_u = 48.58°, t/b = 0.6; **a)** streamlines; **b)** streamlines – enlarged; **c)** exit angles (scale on the left); **d)** changes of exit angle α_1 along datum +5 mm*

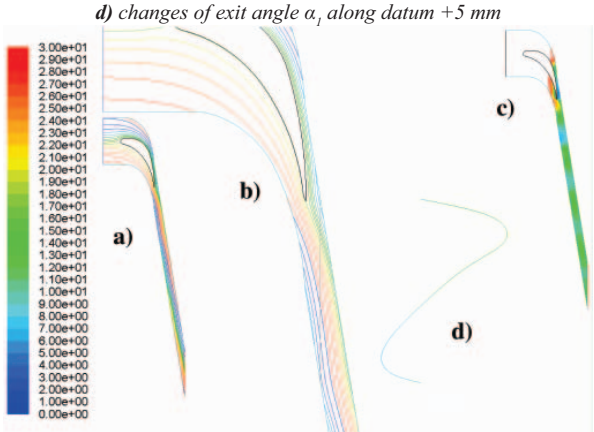

***Fig. 12.** Results of calculations for profile N3-60, α_u = 36.58°, t/b = 0.8; **a)** streamlines; **b)** streamlines – enlarged; **c)** exit angles (scale on the left); **d)** changes of exit angle α_1 along datum +5 mm*

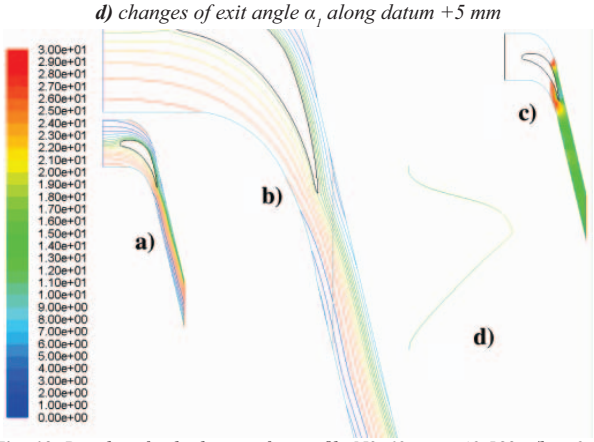

***Fig. 13.** Results of calculations for profile N3-60, α_u = 40.58°, t/b = 0.8; **a)** streamlines; **b)** streamlines – enlarged; **c)** exit angles (scale on the left); **d)** changes of exit angle α_1 along datum +5 mm*

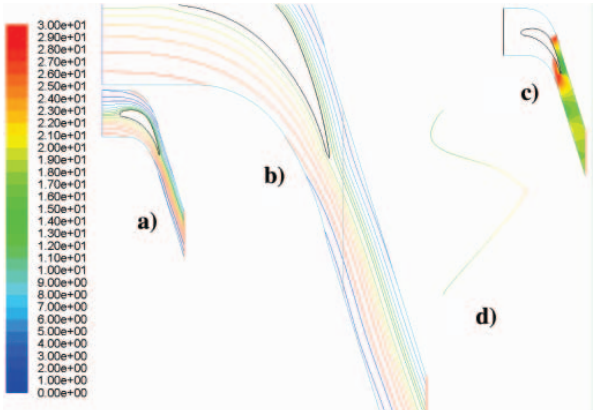

*Fig. 14. Results of calculations for profile N3-60, α_u = 44.58°, t/b = 0.8; **a)** streamlines; **b)** streamlines – enlarged; **c)** exit angles (scale on the left); **d)** changes of exit angle α_1 along datum +5 mm*

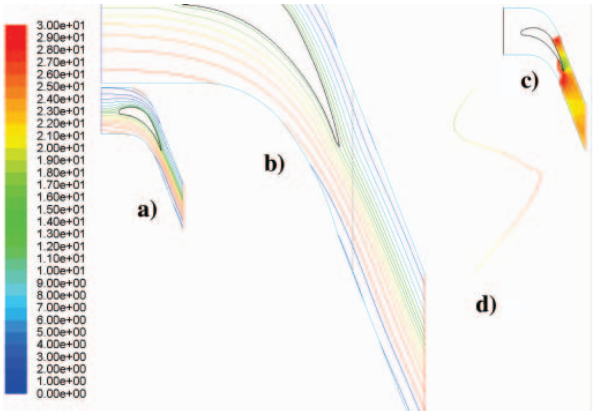

*Fig. 15. Results of calculations for profile N3-60, α_u = 48.58°, t/b = 0.8; **a)** streamlines; **b)** streamlines – enlarged; **c)** exit angles (scale on the left); **d)** changes of exit angle α_1 along datum +5 mm*

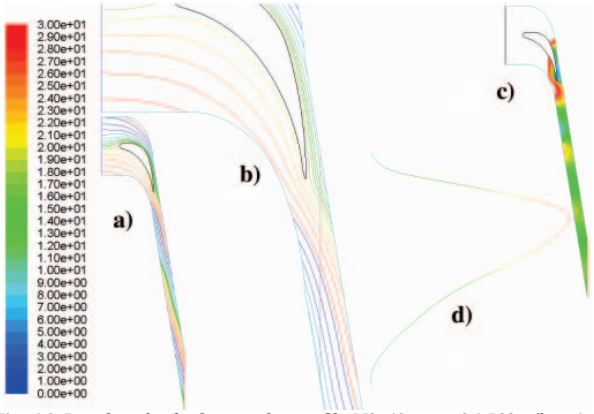

*Fig. 16. Results of calculations for profile N3-60, α_u = 36.58°, t/b = 1.0; **a)** streamlines; **b)** streamlines – enlarged; **c)** exit angles (scale on the left); **d)** changes of exit angle α_1 along datum +5 mm*

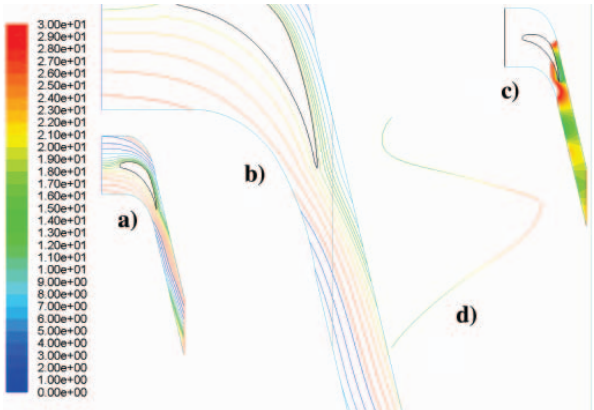

*Fig. 17. Results of calculations for profile N3-60, α_u = 40.58°, t/b = 1.0; **a)** streamlines; **b)** streamlines – enlarged; **c)** exit angles (scale on the left); **d)** changes of exit angle α_1 along datum +5 mm*

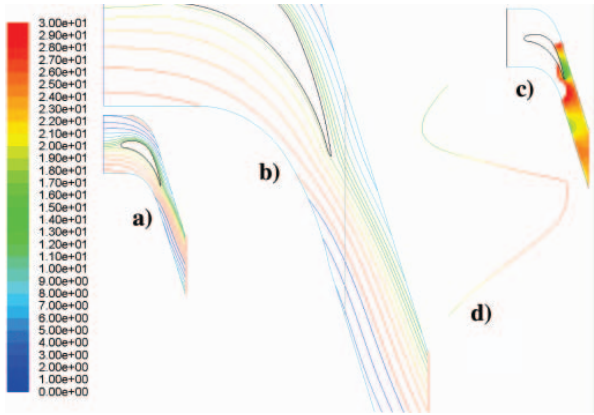

*Fig. 18. Results of calculations for profile N3-60, α_u = 44.58°, t/b = 1.0; **a)** streamlines; **b)** streamlines – enlarged; **c)** exit angles (scale on the left); **d)** changes of exit angle α_1 along datum +5 mm*

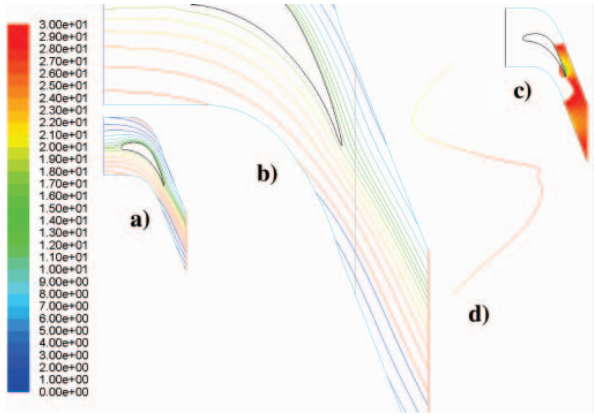

*Fig. 19. Results of calculations for profile N3-60, α_u = 48.58°, t/b = 1.0; **a)** streamlines; **b)** streamlines – enlarged; **c)** exit angles (scale on the left); **d)** changes of exit angle α_1 along datum +5 mm*

COMPARING THE EXPERIMENTAL AND NUMERICAL RESULTS

The measured data presented in [1] include the exit angles α_1 in the form of the diagram shown in Fig. 20. These data were used as the reference for the calculations.

The comparison of the angles α_1 measured experimentally and calculated is given in Fig. 21. For small cascade profile stagger angles α_u, we can observe remarkable dif ferences between the experiment and calculation.

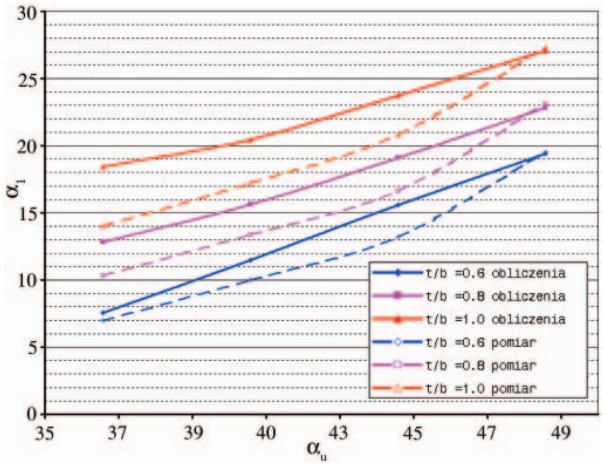

Fig. 21. Comparing exit angles α_1 obtained from measurement and calculations as a function of pitch t/b and stagger angle α_u

From the point of view of impulse turbine flow system calculations these difference are of high significance. For the

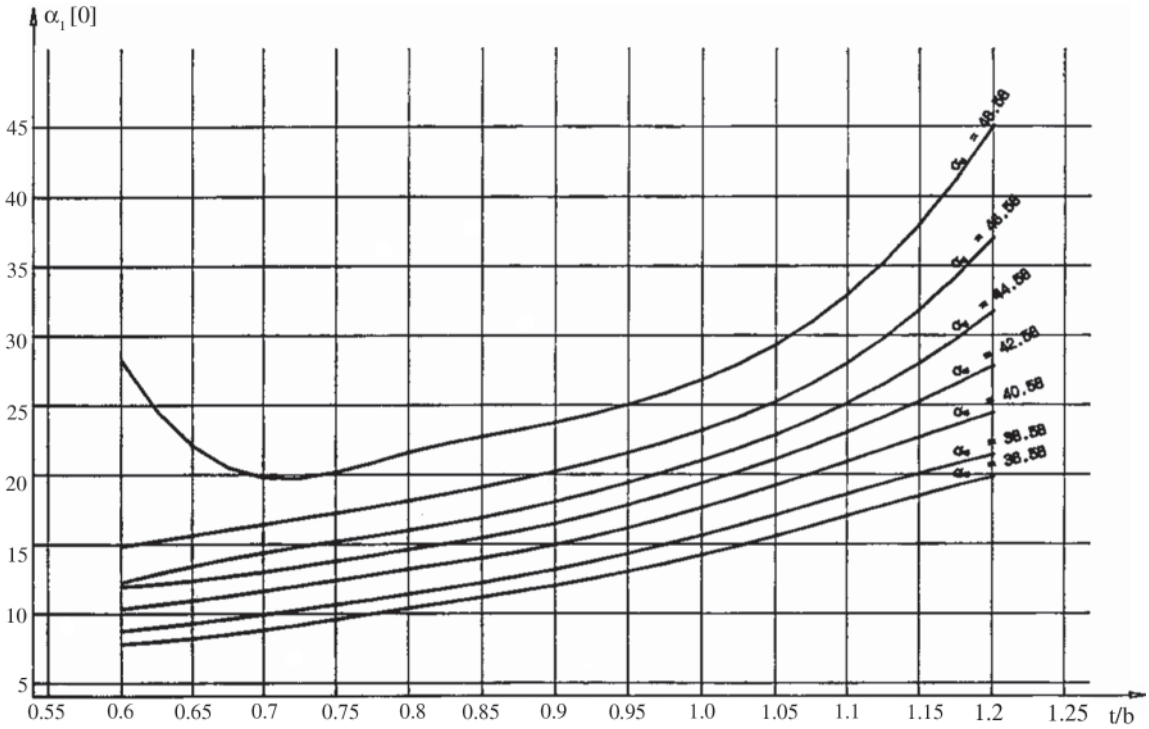

Fig. 20. *Exit angles α_1 for profile cascade N3-60 vs. pitch t/b and stagger angle α_u [1]*

smallest stagger angles (about 36°) this difference approximately equals to 3°. Taking into account that the exit angles in this area are within 12°-15°, the above diference corresponds to an error of an order of 20-30 %, which then leads to a similar error in assessing the mass flow rate though the turbine flow system. To better illustrate this problem, Fig. 22 shows the diferences between the calculated and measured values:

$$\Delta\alpha = \alpha_{1obl} - \alpha_{1pom}$$

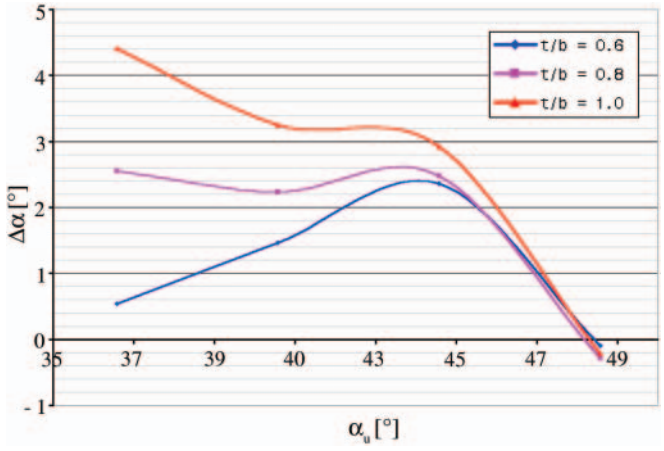

Fig. 22. *Differences between measured and calculated exit angles α_1 vs. pitch t/b and stagger angle α_u*

The diagram in Fig. 22 reveals that for large stagger angles in the N3 cascade, the differences between the measured and calculated angles are negligible. For smaller stagger angles, systematic increase of the dif ference between the calculated and real values is observed. Moreover, a remarkable effect of the cascade pitch on the range of these differences is observed. In extreme cases, for lar ge t/b and small stagger angles the difference between the measured and calculated exit angles can approximately reach as much as 4.5°.

BIBLIOGRAPHY

1. Thermal and flow characteristics of operation of turbine profiles and stages produced in ZAMECH. Report of the Czestochowa University of Technology (in Polish), 1988.
2. FLUENT 6.3 User's Guide, Chapter 11: Modeling Flows Using Sliding and Deforming Meshes.
3. R. Puzyrewski: Analysis of model turbine investigations of cylindrical stages. VIII Conf. on Turbines of Large Output 1984
4. R. Puzyrewski, P. Krzyślak: Parametric analysis of the efficiency function of radial impulse stages (in Polish) – IF-FM Report no. 334/94 – Gdańsk – 1994
5. Dobes, Fort, Halama, Kozel: Numerical simulation of a flow for turbomachinery applications – Con. INTERNAL FLOW – 2001.

CONTACT WITH AUTHORS

Biernacki Rafał, Ph. D.
Faculty of Mechanical Engineering
Gdansk University of Technology
Narutowicza 11/12
80-952 Gdansk, POLAND
e-mail: rbiernac@pg.gda.pl

Piotr Krzyślak, Assoc. Prof.
Faculty of Mechanical Engineering and Management
Poznan University of Technology
Piotrowo 3
60-965 Poznan, POLAND
e-mail: piotr.krzyslak@put.poznan.pl